NASA/TM—2004-213125

Modeling the Nonlinear, Strain Rate Dependent Deformation of Woven Ceramic Matrix Composites With Hydrostatic Stress Effects Included

Robert K. Goldberg and Kelly S. Carney
Glenn Research Center, Cleveland, Ohio

June 2004

The NASA STI Program Office . . . in Profile

Since its founding, NASA has been dedicated to the advancement of aeronautics and space science. The NASA Scientific and Technical Information (STI) Program Office plays a key part in helping NASA maintain this important role.

The NASA STI Program Office is operated by Langley Research Center, the Lead Center for NASA's scientific and technical information. The NASA STI Program Office provides access to the NASA STI Database, the largest collection of aeronautical and space science STI in the world. The Program Office is also NASA's institutional mechanism for disseminating the results of its research and development activities. These results are published by NASA in the NASA STI Report Series, which includes the following report types:

- TECHNICAL PUBLICATION. Reports of completed research or a major significant phase of research that present the results of NASA programs and include extensive data or theoretical analysis. Includes compilations of significant scientific and technical data and information deemed to be of continuing reference value. NASA's counterpart of peer-reviewed formal professional papers but has less stringent limitations on manuscript length and extent of graphic presentations.

- TECHNICAL MEMORANDUM. Scientific and technical findings that are preliminary or of specialized interest, e.g., quick release reports, working papers, and bibliographies that contain minimal annotation. Does not contain extensive analysis.

- CONTRACTOR REPORT. Scientific and technical findings by NASA-sponsored contractors and grantees.

- CONFERENCE PUBLICATION. Collected papers from scientific and technical conferences, symposia, seminars, or other meetings sponsored or cosponsored by NASA.

- SPECIAL PUBLICATION. Scientific, technical, or historical information from NASA programs, projects, and missions, often concerned with subjects having substantial public interest.

- TECHNICAL TRANSLATION. English-language translations of foreign scientific and technical material pertinent to NASA's mission.

Specialized services that complement the STI Program Office's diverse offerings include creating custom thesauri, building customized databases, organizing and publishing research results . . . even providing videos.

For more information about the NASA STI Program Office, see the following:

- Access the NASA STI Program Home Page at ***http://www.sti.nasa.gov***

- E-mail your question via the Internet to help@sti.nasa.gov

- Fax your question to the NASA Access Help Desk at 301–621–0134

- Telephone the NASA Access Help Desk at 301–621–0390

- Write to:
  NASA Access Help Desk
  NASA Center for AeroSpace Information
  7121 Standard Drive
  Hanover, MD 21076

NASA/TM—2004-213125

Modeling the Nonlinear, Strain Rate Dependent Deformation of Woven Ceramic Matrix Composites With Hydrostatic Stress Effects Included

Robert K. Goldberg and Kelly S. Carney
Glenn Research Center, Cleveland, Ohio

National Aeronautics and
Space Administration

Glenn Research Center

June 2004

Available from

NASA Center for Aerospace Information
7121 Standard Drive
Hanover, MD 21076

National Technical Information Service
5285 Port Royal Road
Springfield, VA 22100

Available electronically at http://gltrs.grc.nasa.gov

Modeling the Nonlinear, Strain Rate Dependent Deformation of Woven Ceramic Matrix Composites With Hydrostatic Stress Effects Included

Robert K. Goldberg and Kelly S. Carney
National Aeronautics and Space Administration
Glenn Research Center
Cleveland, Ohio 44135

Summary

An analysis method based on a deformation (as opposed to damage) approach has been developed to model the strain rate dependent, nonlinear deformation of woven ceramic matrix composites with a plain weave fiber architecture. In the developed model, the differences in the tension and compression response have also been considered. State variable based viscoplastic equations originally developed for metals have been modified to analyze the ceramic matrix composites. To account for the tension/compression asymmetry in the material, the effective stress and effective inelastic strain definitions have been modified. The equations have also been modified to account for the fact that in an orthotropic composite the in-plane shear stiffness is independent of the stiffness in the normal directions. The developed equations have been implemented into a commercially available transient dynamic finite element code, LS-DYNA, through the use of user defined subroutines (UMATs). The tensile, compressive, and shear deformation of a representative plain weave woven ceramic matrix composite are computed and compared to experimental results. The computed values correlate well to the experimental data, demonstrating the ability of the model to accurately compute the deformation response of woven ceramic matrix composites.

Introduction

Ceramic matrix composites are gaining wider usage in the aerospace industry due to their ability to withstand high temperatures while still providing relatively high stiffness and strength levels as compared to monolithic ceramics. Woven ceramic matrix composites with a 2–D plane weave fiber architecture are commonly used due to their ability to provide high levels of stiffness and strength in multiple directions. One area of interest to NASA is studying how these materials respond to high strain rate impact loads. However, these ceramic composites have several characteristics in the macroscopic deformation response which make modeling the deformation response under impact conditions challenging. The stress-strain curve for these materials are nonlinear, particularly in tension and shear, due to factors such as matrix microcracking (refs. 1 and 2), and the deformation response changes with strain rate (refs. 3 and 4). Furthermore, the uniaxial tension and compression responses are different (refs. 1 and 5), which implies that on the macroscopic scale the hydrostatic stresses have an effect on the material response.

Previous efforts have focused on using damage mechanics approaches to model the nonlinear deformation of woven ceramic matrix composites (refs. 1,5, and 6). However, there are several features of these models which indicate that examining alternative methods of simulating the material response would be beneficial. First of all, in these previous models strain rate dependence of the material behavior is not explicitly accounted for within the model. However, previous studies on these materials (refs. 3 and 4) have indicated that these materials indeed have a nontrivial rate dependence. Furthermore, in the previous studies referenced above all of the nonlinearity of the deformation response is assumed to

be due to damage mechanisms instead of deformation mechanisms. Providing an alternative modeling capability in which the nonlinearity in the deformation response is assumed to be due to deformation mechanisms could allow for a decoupling of the deformation and damage/failure response, which could facilitate improved modeling of both the deformation response and the prediction of ultimate failure.

At NASA Glenn Research Center, efforts have been underway for several years to model the strain rate dependent, nonlinear deformation of polymers with the effects of hydrostatic stresses included. In these efforts, the Bodner-Partom viscoplasticity model based on the state variable approach (ref. 7), originally developed for metals, has been modified in order to incorporate the hydrostatic stress effects known to be present in polymers (ref. 8). These variations include modifying the effective stress and effective inelastic strain definitions, based on an application of the Drucker-Prager yield criterion (ref. 9), to account for the effects of the hydrostatic stresses.

In this paper, the constitutive equations with an associative flow rule mentioned above have been applied and modified in order to model the nonlinear, strain rate dependent, deformation of plain weave woven ceramic matrix composites, in which the differences in the tensile and compressive response are accounted for within the equations. Due to the plain weave fabric geometry of the materials, for the purposes of this study the material is assumed to be isotropic in the normal directions, even though these materials are composites and not homogenous materials. However, since the woven composites are indeed orthotropic materials on the macroscopic level, the shear response is assumed to be uncoupled from and independent of the normal response. The full theoretical development of the constitutive equations will be described in this paper, along with the procedures to be used to determine the material constants. The procedures used to implement the equations within a commercially available transient dynamic finite element code, LS-DYNA (ref. 10), through the use of user defined subroutines will also be described. Finally, the tensile, compressive, and shear deformation of a representative plain weave woven ceramic matrix composite will be computed and compared to experimental results to demonstrate the ability of the model to capture the features of the deformation response of plain weave woven ceramic matrix composite materials.

Theoretical Development

To analyze the nonlinear, strain rate dependent deformation of plain weave woven ceramic matrix composites, the Bodner-Partom viscoplastic state variable model (ref. 7), which was originally developed to analyze the viscoplastic deformation of metals above one-half of the melting temperature and has been successfully used in such instances, has been modified. This particular model was chosen due to previous success in using a variation of this model to analyze the strain rate dependent, nonlinear deformation of polymer materials (ref. 8). In state variable models, a single unified strain variable is defined to represent all inelastic strains (ref. 11). Furthermore, in the state variable approach there is no defined yield stress. Inelastic strains are assumed to be present at all values of stress, the inelastic strains are just assumed to be very small in the “elastic” range of deformation. State variables, which evolve with stress and inelastic strain, are defined to represent the average effects of the deformation mechanisms.

An important point to note is that frequently, in state variable models, each of the state variables and material constants have a fairly explicit link to specific deformation mechanisms, such as dislocation pileups in metals (ref. 11). Here, due to the complex nature of the material deformation mechanisms in woven ceramic matrix composites the linkage between the state variables and material constants to specific deformation mechanisms is not nearly as well defined. For this work, an internal stress state variable is defined to represent phenomelogically the resistance to inelastic deformation, a state variable is defined to represent the effects of hydrostatic stresses and a state variable is defined in order to scale the shear stresses to ensure a consistent effective stress. The material constants are characterized in order to correlate with the experimentally observed deformation of the material, and are not tightly linked to specific deformation mechanisms. However, the equations developed here employ a fairly simple

formulation with a minimum of material constants that are fairly simple to characterize, and capture the main features of the deformation response.

For this study, temperature and moisture effects have been neglected, as only room temperature data are currently available. All of the nonlinearity and strain rate dependence observed in the material is assumed in this work to be due to inelastic deformation, where in reality the nonlinearity is most likely due to a mixture of deformation and damage. Ultimate damage and failure criteria will need to be added to the model at a later date. Small strain theory is assumed to apply, and phenomena such as creep, relaxation and high cycle fatigue are not accounted for within the equations. Furthermore, as mentioned previously, in reality plain weave woven ceramic matrix composites are orthotropic materials, as is typical of composites. However, due to the plain weave architecture of the fibers, the material can be assumed to be isotropic in the normal directions, with independent shear responses.

Associated Flow Equation and Evolution Equations

In order to derive the associated flow equation for the components of the inelastic strain rate tensor for plain weave woven ceramic matrix composites with hydrostatic stress effects (different responses in tension and compression) included, a procedure similar to that employed to derive the Prandtl-Reuss equations in classical plasticity is utilized (refs. 9 and 11). The formulation employed in this study is based on that used by Pan and co-workers (refs. 12 and 13) and Hsu, et al (ref. 14). First, an inelastic potential function based on the Drucker-Prager yield criterion (ref. 9) is defined as

$$f = \sqrt{J_2^*} + \alpha\sigma_{kk} \tag{1}$$

where σ_{kk} is the sum of the normal stress components (assuming the usual rules of indicial notation (ref. 11)) and is equal to three times the hydrostatic stress. The variable α is a state variable which controls the level of the hydrostatic stress effects. The term "$\alpha\sigma_{kk}$" incorporates the effects of hydrostatic stresses into the inelastic potential function. The variable J_2^* is a modified version of the second invariant of the deviatoric stress tensor. The modification is required due to the fact that for the orthotropic composites examined here, the shear terms are independent of the normal terms in the stiffness matrix. Therefore, in order to ensure a consistent effective stress (meaning a constant effective stress vs. effective strain curve independent of the load type), the shear stresses must be multiplied by a scaling state variable β. The modified version of the deviatoric second invariant is given as follows

$$J_2^* = \frac{1}{6}\left[(\sigma_{11}-\sigma_{22})^2 + (\sigma_{22}-\sigma_{33})^2 + (\sigma_{33}-\sigma_{11})^2\right] + \beta\left[\sigma_{12}^2 + \sigma_{13}^2 + \sigma_{23}^2\right] \tag{2}$$

where σ_{ij} are the components of the stress tensor. Note that for the current work all three shear stress components are scaled by the same value of β. In actuality, each shear stress component may require a unique scaling factor. However, for the current work only in-plane loads are considered, and in the finite element implementation the model is applied using thin shell elements only at the current time, which results in the transverse shear stresses being approximate at best. Furthermore, at the current time only in-plane shear data is available to be examined. As a result, only the correct scaling of the in-plane shear stresses is considered significant for this work. The effects of possible errors in the scaling of the transverse shear stresses are not considered at this time. The full effects of the transverse shear stresses will be considered in future work.

The components of the inelastic strain rate tensor, $\dot{\varepsilon}_{ij}^{I}$, are assumed to be proportional to the derivative of the potential function with respect to the components of the stress tensor, σ_{ij}, as follows

$$\dot{\varepsilon}_{ij}^{I} = \dot{\lambda}\frac{\partial f}{\partial \sigma_{ij}} \tag{3}$$

where $\dot{\lambda}$ is a scalar rate variable. By taking the specified derivative of the potential function, the result becomes

$$\frac{\partial f}{\partial \sigma_{ij}} = \frac{S_{ij}^{*}}{2\sqrt{J_2}} + \alpha\delta_{ij} \tag{4}$$

where δ_{ij} is the Kronecker delta and S_{ij}^{*} are the modified components of the deviatoric stress tensor. For the normal stress components, S_{ij}^{*} is equal to S_{ij}, the components of the deviatoric stress tensor. However, to maintain consistency, for the shear stress components the terms are scaled as follows

$$S_{ij}^{*} = \left(\sqrt{\beta}\right)\sigma_{ij} \tag{5}$$

where β is the shear scaling state variable discussed earlier.

The next step in defining the flow rule is to define the effective stress and the effective inelastic strain rate. The effective stress, σ_e, is defined as follows

$$\sigma_e = \sqrt{3}f = \sqrt{3J_2^{*}} + \sqrt{3}\alpha\sigma_{kk}\,. \tag{6}$$

To determine the value of the scalar $\dot{\lambda}$ in terms of the effective inelastic strain rate, $\dot{\varepsilon}_e^{I}$, the principal of the equivalence of the inelastic work rate is employed. With the aid of equations (3) and (4), the inelastic work rate, $\dot{W}^{I}$, can be expressed by the following

$$\dot{W}^{I} = \sigma_{ij}\dot{\varepsilon}_{ij}^{I} = \sigma_{ij}\left(\frac{S_{ij}^{*}}{2\sqrt{J_2}} + \alpha\delta_{ij}\right)\dot{\lambda} = \sigma_e\dot{\varepsilon}_e^{I}\,. \tag{7}$$

After applying the effective stress definition given in equation (6) and simplifying, it can be shown that

$$\dot{\lambda} = \sqrt{3}\dot{\varepsilon}_e^{I} \tag{8}$$

By substituting equation (8) and equation (4) into equation (3), a definition for the components of the inelastic strain rate tensor can be given as

$$\dot{\varepsilon}_{ij}^{I} = \sqrt{3}\dot{\varepsilon}_e^{I}\left(\frac{S_{ij}^{*}}{2\sqrt{J_2}} + \alpha\delta_{ij}\right). \tag{9}$$

By utilizing equation (7), it can be shown that the effective inelastic strain rate can be defined as

$$\dot{\varepsilon}_e^I = \dot{e}_e^I = \sqrt{\frac{2}{3}\left[\left(\dot{e}_{11}^I\right)^2 + \left(\dot{e}_{22}^I\right)^2 + \left(\dot{e}_{33}^I\right)^2\right] + \frac{4}{3}\kappa^2\left[\left(\dot{e}_{12}^I\right)^2 + \left(\dot{e}_{13}^I\right)^2 + \left(\dot{e}_{23}^I\right)^2\right]}$$
$$\dot{e}_{ij}^I = \dot{\varepsilon}_{ij}^I - \dot{\varepsilon}_m^I \delta_{ij} \tag{10}$$

where $\dot{e}_e^I$ is the effective deviatoric inelastic strain rate and $\dot{\varepsilon}_m^I$ is the mean inelastic strain rate. The inelastic shear strain rates need to be scaled by a constant scale factor κ due to the fact that for an orthotropic material the shear terms in the material response are independent of the normal terms. When κ equals one, which would happen for isotropic materials, the inelastic strain rate definition given here matches the effective inelastic strain rate definition given by Pan and co-workers (refs. 12 and 13).

By following a similar format to the Bodner-Partom model (refs. 7 and 11), the following definition is specified

$$\frac{\sqrt{3}}{2}\dot{\varepsilon}_e^I = D_o \exp\left[-\frac{1}{2}\left(\frac{Z}{\sigma_e}\right)^{2n}\right] \tag{11}$$

where D_o and n are material constants. D_o represents the maximum inelastic strain rate, and n controls the rate dependence of the material. Z is an isotropic state variable which represents the resistance to inelastic deformation (internal stress). By substituting equation (11) into equation (9), the final form of the flow equation is determined to be

$$\dot{\varepsilon}_{ij}^I = 2D_o \exp\left[-\frac{1}{2}\left(\frac{Z}{\sigma_e}\right)^{2n}\right]\left(\frac{S_{ij}}{2\sqrt{J_2}} + \alpha\delta_{ij}\right). \tag{12}$$

Note that the elastic components of the strain rate must be added to the inelastic strain rate to obtain the total strain rate.

The rate of evolution of the internal stress state variable Z, the hydrostatic stress effect state variable α and the shear scaling factor state variable β are defined by the equations

$$\dot{Z} = q(Z_1 - Z)\dot{e}_e^I \tag{13}$$

$$\dot{\alpha} = q(\alpha_1 - \alpha)\dot{e}_e^I \tag{14}$$

$$\dot{\beta} = q(\beta_1 - \beta)\dot{e}_e^I \tag{15}$$

where q is a material constant representing the "hardening" rate, and Z_1, α_1, and β_1 are material constants representing the maximum values of Z, α, and β respectively. The initial values of Z, α, and β are defined by the material constants Z_o, α_o and β_o. The term $\dot{e}_e^I$ in equations (13), (14), and (15) represents the effective deviatoric inelastic strain rate, which was defined in equation (10). An important point to note is that in the original Bodner model (ref. 7), the inelastic work rate was used instead of the effective inelastic strain rate in the evolution equation for the internal stress state variable. However, for this work the inelastic strain rate was deemed easier to work with from both computational and characterization points of view, particularly in the incorporation of hydrostatic stress effects. Furthermore, the effective inelastic strain rate has been used in other state variable constitutive models (ref. 11). Since hydrostatic stress

effects were not considered in the original Bodner model (ref. 7), the evolution equation for α is new to this work. Furthermore, since these equations were originally developed for homogenous isotropic materials and not composites, the evolution equation for β is also new to this work. The state variables α and β are assumed to evolve in the same manner as the state variable Z. By using this assumption the value of q used in equations (14) and (15) can be shown to be the same as the value of q used in equation (13).

Determination of Material Constants

The material constants that need to be determined include D_0, n, Z_o, Z_1, α_o, α_1, β_o, β_1, κ, and q. These values, along with the elastic modulus, shear moduli and Poisson's ratio are the input parameters required for the model. The procedure to be used is summarized here. More details on the procedure as it was used for isotropic polymers can be found in Goldberg, et al. (ref. 8). The constants are determined using tensile and compressive stress-strain curves obtained from a set of constant strain rate tests, along with a shear stress-shear strain curve obtained for at least one strain rate. Each tension and compression test is conducted at a different total strain rate.

The first step in the process is to obtain the values of α_1 and α_o. To accomplish this task, equation (6) is used in combination with stress-strain data from constant strain rate uniaxial tension and compression tests. The values of these constants are assumed to be rate independent, so the results from only one strain rate need to be used to find the needed parameters. In practical application of the methodology, the uniaxial tension and compression tests used do not have to be at the exact same effective strain rate. As long as the effective strain rates from the two tests are approximately equal, the values obtained have been found to be valid, particularly if quasi-static strain rates are examined. Two stress values from the tensile and compressive stress-strain curves are required in order to find these two constants. First of all, the "saturation stress", the stress level at which the stress-strain curve flattens out and becomes horizontal, is required. At this stress level, the inelastic strain rate is assumed to be equal to the total applied strain rate. If the actual stress-strain curve terminates before the saturation stress is reached (as often happens in compression), the curve must be extrapolated to obtain an approximate value of the saturation stress. Secondly, the stress level at which the tension and compression curves becomes nonlinear (the "yield" stress), is required. One important point needs to be considered when determining the stress level designating the onset of nonlinearity. Frequently, in woven ceramic matrix composites, the tensile stiffness across nearly the entire stress-strain curve tends to be significantly softer than the compressive stiffness, most likely due to the fact that in tension significant matrix microcracks develop almost immediately upon loading, which weakens the material. As a result, in cases where this phenomena occurs the initial portion of the compression curve is assumed to represent the "elastic" regime of the composite material, and in tension the onset of nonlinearity in the stress-strain curve is assumed to occur at a very small, almost negligible stress value.

Given these definitions, equation (6) can now be used to determine the values of α_1 and α_o. The primary assumption used at this point (and assumed implicitly in equation (6)) is that the effective stress at saturation under uniaxial tensile loading at a particular strain rate is equal to the effective stress at saturation under compression loading at the same equivalent strain rate. Likewise, the effective stress at the point the stress-strain curve becomes nonlinear under tensile loading is equal to the effective stress at the point the stress-strain curve becomes nonlinear under compression loading. Therefore, assuming the value of α at saturation is equal to α_1, and the value of α at the point the stress-strain curve becomes nonlinear is equal to α_o, the following equations are obtained for the case of having data from uniaxial tension and compression tests

$$\sigma_{st}\left(1+\sqrt{3}\alpha_1\right)=\sigma_{sc}\left(1-\sqrt{3}\alpha_1\right) \tag{16}$$

$$\sigma_{nlt}\left(1+\sqrt{3}\alpha_o\right)=\sigma_{nlc}\left(1-\sqrt{3}\alpha_o\right) \tag{17}$$

where σ_{st} and σ_{sc} are the tensile and compressive stresses at saturation, respectively, and σ_{nlt} and σ_{nlc} are the tensile and compressive stresses at the point where the respective stress-strain curves become nonlinear. Therefore, by substituting the tensile and compressive stresses at saturation into this equation, followed by the tensile and compressive stresses at the point where the respective stress-strain curves become nonlinear, the required constants can be determined. At this point, by applying equation (6) for the tensile and shear curves, using the appropriate "saturation" and "yield" stresses in tension and shear, the values of β_o and β_1 can be determined from the following equations

$$\sigma_{st}\left(1+\sqrt{3}\alpha_1\right)=\sqrt{3\beta_1}\tau_s \tag{18}$$

$$\sigma_{nlt}\left(1+\sqrt{3}\alpha_o\right)=\sqrt{3\beta_o}\tau_{nl} \tag{19}$$

where σ_{st} and τ_s are the tensile and shear stresses at saturation, respectively, and σ_{nlt} and τ_{nl} are the tensile and shear stresses at the point where the respective stress-strain curves become nonlinear.

The values of D_0, n, and Z_1 are characterized as follows. The value of D_0 is currently assumed to be equal to a value of 10^4 times the maximum applied strain rate, which correlates with the maximum inelastic strain rate. To determine the values of n and Z_1, first equation (12) is simplified to the case of uniaxial tensile loading, leading to the following expression

$$\dot{\varepsilon}^I = 2D_0 \exp\left[-\frac{1}{2}\left(\frac{Z}{(1+\sqrt{3}\alpha)\sigma}\right)^{2n}\right]\left(\frac{\sigma}{\sqrt{3}|\sigma|}+\alpha\right) \tag{20}$$

where $\dot{\varepsilon}^I$ is the uniaxial tensile inelastic strain rate in a constant strain rate tensile test, σ is the uniaxial tensile stress, and the remainder of the terms are as defined earlier. The case of uniaxial tensile loading is used to determine these constants since for woven ceramic matrix composites the tensile stress-strain curves obtained experimentally are more likely to display a defined "saturation" stress than the compression curves, which as shown below is crucial for determining the material constants. Furthermore, equation (20) can be rearranged as follows

$$-2\ln\left(\frac{\dot{\varepsilon}^I}{2D_0\left(\frac{1}{\sqrt{3}}+\alpha\right)}\right)=\left(\frac{Z}{(1+\sqrt{3}\alpha)\sigma}\right)^{2n}. \tag{21}$$

The required constants are determined from a set of tensile stress-strain curves obtained from constant strain rate tests. Each curve in this set is obtained at a different constant strain rate. Data pairs of the total strain rate (equal to the inelastic strain rate at saturation) and saturation stress values from each curve are taken. For each strain rate, the data values are substituted into equation (21), after the natural logarithm of both sides of the equation is taken, and represent a point on a master curve. The number of points in the master curve equals the number of strain rates at which the tensile tests were conducted. A least squares regression analysis is then performed on the master curve. As can be shown from equation (21), the slope of the best-fit line is equal to $-2n$. The intercept of the best-fit line is equal to $2n(ln(Z_1))$.

To determine the value of Z_o, equation (21) can be used again. In this case, the value of the tensile stress where the stress-strain curve becomes nonlinear for a particular constant strain rate tensile test is

used, as well as the value of the approximate inelastic strain rate when the stress-strain curve becomes nonlinear. The point where the stress-strain curve becomes nonlinear is defined as the approximate point where the curve appreciably deviates from a linear extrapolation of the initial data. The strain rate used in the constant strain rate test divided by 100 was found by trial and error to approximate the inelastic strain rate at this point reasonably well. Using this data, equation (21) is solved for Z, which is assumed to be equal to the value of Z_o. Compression data can also be used, particularly for the case when the tensile stress at which the stress-strain curve becomes nonlinear is approximated due to the differences in the initial tension and compression responses as discussed above. In this case, equations (20) and (21) need to be reformulated based on equation (12) given that compressive stresses are being considered as opposed to tensile stresses. Another point to note is that using the data from the lowest strain rate test available has been found to give adequate values of Z_o. However, the calculations can be made using data from all the available strain rates, and an average taken if required to obtain the value of the constant.

To determine the value for q for equations (13), (14), and (15), first equation (13) is integrated for the case of pure tensile loading (again since for woven ceramic matrix composites the tensile curves are more likely to display a distinct saturation stress), resulting in the following relation

$$Z = Z_1 - (Z_1 - Z_o)\exp\left(-q\varepsilon_e{}^I\right) \tag{22}$$

where $\varepsilon_e{}^I$ is the effective inelastic strain, computed using equation (10). At saturation, the value of the internal stress Z is assumed to approach Z_1, resulting in the exponential term approaching zero. Assuming that saturation occurs when the following condition is satisfied

$$\exp\left(\frac{-q\varepsilon_s^I}{1+\sqrt{3}\alpha_1}\right) = 0.01 \tag{23}$$

the equation is solved for q, where $\varepsilon_s{}^I$ is the inelastic tensile strain at saturation. Also, in equation (23) the effective inelastic strain at saturation is simplified to the case of uniaxial tensile loading through the use of equations (9) and (10). If the inelastic strain at saturation is found to vary with strain rate, the parameter q is computed at each strain rate and regression techniques are utilized to determine an expression for the variation of q. If equations (14) and (15) are integrated, an expression similar to equation (23) is obtained. At saturation, the values of α and β are assumed to approach α_1 and β_1, and equations identical to equation (23) are obtained, which would lead to the same value for q. Therefore, identical values of q are used in equations (13), (14), and (15).

To find the value of κ, equation (10) is used along with results from a uniaxial tensile test and a pure shear test. Specifically, the effective inelastic strain at saturation for a tensile test at a particular total strain rate (usually the lowest) is set equal to the effective inelastic strain at saturation from a pure shear test at the same approximate total strain rate, resulting in the following expression which can be solved for κ

$$\frac{\varepsilon_s^I}{1+\sqrt{3}\alpha_1} = \frac{\kappa\gamma_s^I}{\sqrt{3}} \tag{24}$$

where $\varepsilon_s{}^I$ is once again the inelastic tensile strain at saturation and $\gamma_s{}^I$ is the inelastic engineering shear strain at saturation.

Finite Element Implementation

The constitutive equations described above have been implemented into the commercially available transient dynamic finite element code LS-DYNA (ref. 10) through the use of the user defined subroutine (UMAT) option. For this work, the user defined routine was designed to work with shell elements, therefore the equations were specialized for the case of plane stress in the normal directions. A composite is typically a thin structure, which justifies the use of shell elements. The use of shell elements also allows greater flexibility in terms of defining a laminate of many composite plies, and in specifying the angle of orientation of the material. Furthermore, the use of shell elements provides greater flexibility and computational efficiency in terms of analyzing a complex structure. All of the material constants are entered into the input deck. The current values of the stress and any history variables at time t, along with the strain increments in progressing from time t to time $t + \Delta t$, are passed into the routine by LS-DYNA. The stresses and values of the history variables at time $t + \Delta t$ are to be computed within the routine. The history variables for the finite element analysis are defined to include the deviatoric stresses, the hydrostatic stress, the values of the state variables and the inelastic strain rate tensor. To integrate the constitutive equations, a fourth order Runge-Kutta integrator (ref. 15) has been implemented into the UMAT routines. For this class of problems, implicit integration routines have often been used because of their inherent numerical stability (ref. 11). However, in transient dynamic finite codes, explicit integration schemes are employed so an explicit integrator was required for the user defined subroutine developed in this work.

In the UMAT routine, the material constants and the current values of the history variables are read into the routine. The values of the elastic stiffness tensor are computed based on the elastic modulus and Poisson's ratio. For each step of the Runge-Kutta integration, the effective stress is computed employing the current stress values and the current value of the state variables α and β using equation (6). Next, the terms in the inelastic strain rate tensor are determined using equation (12). The effective inelastic strain rate is determined using equation (10), and then the state variable rates are determined using equations (13), (14), and (15). The appropriate integration formula and time step increment based on the progress through the Runge-Kutta integration routine is then used to compute updated values of the inelastic strain increments and the state variables. From the given total strain increments and the computed inelastic strain increments, along with the elastic constants, the values which are computed include the strain increments for the current step in the integration process, the stress increments and revised total stresses. In this process, the out of plane normal strain increments are calculated in a manner such that the plane stress condition is enforced, and the out of plane normal stress is set equal to zero. As is common for shell elements, a correction factor of 0.833 (ref. 10) is used in computing the transverse shear stresses. Revised values of the deviatoric and hydrostatic stresses determined from the computed stresses, and the integration process is continued as required. Finally, the history variables are updated, and the routine returns.

Sample Calculations

To demonstrate the ability of the developed constitutive equations to correctly simulate the nonlinear deformation response of woven ceramic matrix composites, a representative plain weave woven SiC/SiC system, with a Tyranno fiber in a SiC matrix, was analyzed. The experimental data were obtained by Jacobsen and Brondsted (ref. 5), in which the details of the material and the experimental procedures can be found. Tensile, compressive and in-plane shear stress-strain curves obtained at a quasi-static strain rate and room temperature are shown in figures 1, 2, and 3, respectively. The tensile and compressive results were measured along the fiber direction. As can be seen in the figures, the compression stress-strain curve is nearly linear elastic until failure, with only a slight nonlinearity. However, the tensile curve is highly nonlinear, due to matrix microcracking and interfacial debonding, and has a much lower failure stress

than the compression results. The stress-strain curve in shear also displays significant amounts of nonlinearity.

To determine the material constants for the constitutive equations described in the previous section, the elastic and shear modulus, Poisson's ratio, yield stress (stress where the stress-strain curve becomes nonlinear) in tension, compression and shear, saturation stress (stress level where the stress-strain curves becomes horizontal) in tension, compression and shear, and saturation strain in tension and shear were determined from the material data. The Poisson's ratio data was obtained from Jacobson and Brondsted (ref. 5). This information is presented in table 1. Note that the saturation strain in shear is the engineering shear strain. Also note that since the tension and compression curves did not display a distinct saturation stress, curve extrapolation techniques were used to estimate the saturation stress and strain values. Using the information given in table 1 and the procedures described in previous sections of this paper, the material constants for the constitutive equations were calculated and are shown in table 2. Since strain rate dependent data were not available for this material, based on trends observed in other reports (refs. 3 and 4) a tensile saturation stress of 370 MPa was assumed at a strain rate of 0.1 /sec. The quasi-static test data was assumed to be obtained at a strain rate of 5×10^{-5} /sec.

Computed tension, compression and shear stress-strain curves are shown in figures 1, 2, and 3, respectively, along with the experimental curves for comparison. As can be seen in the figures, the correlation between the experimental and computed results is quite good for all three conditions. Qualitatively, the nonlinearity observed in the tension and shear curves is captured, and the significant differences in the tension and compression responses are correctly captured. Quantitatively, the tensile stresses are slightly under predicted in the early portion of the nonlinear range of the curve, and the shear stresses are slightly over predicted at higher shear strains until saturation is reached, but the differences are not significant. Since strain rate dependent data were not available for this material, in order to explore the capability of the equations to simulate a rate dependent response, a tensile curve was generated at a strain rate of 0.1 /sec, and is shown in figure 4 ("high rate" in the figure) along with the quasi-static computed tensile curve ("low rate" in the figure) for comparison. As can be seen in the figure, the equations do predict a noticeable rate dependence to the tensile response, which indicates that the current model can capture the rate dependence in the material deformation. Future efforts will include obtaining strain rate dependent material data for a woven ceramic matrix composite and more thoroughly examining the capability of the equations to correctly simulate the observed rate dependence in the composite deformation.

Conclusions

The Bodner-Partom viscoplastic state variable model (ref. 7) has been modified in order to analyze the strain rate dependent, nonlinear deformation of plain weave woven ceramic matrix composites. The differences in the tensile and compressive deformation responses have been accounted for through the modification of the effective stress and effective inelastic strain definitions given in the original equations. The procedures used to compute the shear response have also been modified to account for the fact that in an orthotropic composite the shear response is independent of the normal response. The material constants can be obtained based on tension, compression and shear tests. The constitutive equations have been implemented within the transient dynamic finite element code LS-DYNA through the use of the user defined subroutine (UMAT) option. Sample calculations have been conducted using a representative material which demonstrates the ability of the model to qualitatively capture the nonlinearity, strain rate dependence and tension/compression asymmetry observed in the deformation response of woven ceramic matrix composites.

Future efforts will be concentrated in several areas. Primarily, failure criteria will be developed and added to the model, in order to provide the ability to model the full deformation, damage and failure of woven ceramic matrix composites. In addition, as mentioned above the proper modeling of the transverse stresses will be considered in greater detail.

References

1. Camus, G.: "Modeling of the mechanical behavior and damage processes of fibrous ceramic matrix composites: application to a 2-D SiC/SiC." International Journal of Solids and Structures, vol. 37, pp. 919–942, 2000.
2. Camus, G.: Guillaumat, L.; and Baste, S.: "Development of Damage in a 2D Woven C/SiC Composite Under Mechanical Loading: I. Mechanical Characterization." Composites Science and Technology, vol. 56, pp. 1363–1372, 1996.
3. Zhu, S.; Cao, J.-W.; Mizuno, M.; and Kagawa, Y.: "Effect of loading rate and temperature on monotonic tensile behavior in an enhanced SiC/SiC composite." Scripta Materialia, vol. 50, pp. 349–352, 2004.
4. Lipetzky, P.; Dvorak, G.J.; and Stoloff, N.S.: "Tensile properties of a SiC_f/SiC composite." Materials Science and Engineering, vol. A216, pp. 11–19, 1996.
5. Jacobson, T.K.; and Brondsted, P.: "Mechanical Properties of Two Plain-Woven Chemical Vapor Infiltrated Silicon Carbide-Matrix Composites." Journal of the American Ceramic Society, vol. 84, pp. 1043–1051, 2001.
6. Gasser, A.; Ladeveze, P.; and Poss, M.: "Damage Mechanisms of a Woven SiC/SiC Composite: Modeling and Identification." Composites Science and Technology, vol. 56, pp. 779–784, 1996.
7. Bodner, S.R.: Unified Plasticity for Engineering Applications. Kluwer Academic/Plenum Publishers, New York, 2002.
8. Goldberg, R.K.; Roberts, G.D.; and Gilat, A: "Implementation of an Associative Flow Rule Including Hydrostatic Stress Effects Into the High Strain Rate Deformation Analysis of Polymer Matrix Composites." NASA TM-2003-212382, National Aeronautics and Space Administration, 2003.
9. Khan, A.S.; and Huang, S.: Continuum Theory of Plasticity. John Wiley and Sons, Inc., New York, 1995.
10. Anonymous: LS-DYNA Keyword User's Manual, Version 970. Livermore Software Technology Corporation, Livermore, CA, 2003.
11. Stouffer, D.C.; and Dame, L.T.: Inelastic Deformation of Metals. Models, Mechanical Properties and Metallurgy. John Wiley and Sons, New York, 1996.
12. Li, F.Z; and Pan, J.: "Plane-Stress Crack-Tip Fields for Pressure-Sensitive Dilatant Materials." Journal of Applied Mechanics, vol. 57, pp. 40–49, 1990.
13. Chang, W.J.; and Pan, J.: "Effects of Yield Surface Shape and Round-Off Vertex on Crack-Tip Fields for Pressure-Sensitive Materials." International Journal of Solids and Structures, vol. 34, pp. 3291–3320, 1997.
14. Hsu, S.-Y., Vogler, T.J.; and Kyriakides, S.: "Inelastic behavior of an AS4/PEEK composite under combined transverse compression and shear. Part II: modeling." International Journal of Plasticity, vol. 15, pp. 807–836, 1999.
15. Kreyszig, E.: Advanced Engineering Mathematics, 7th Edition. John Wiley and Sons, Inc., New York, 1992.

TABLE 1.—MATERIAL DATA TO BE USED IN DETERMINING MODEL CONSTANTS

	Modulus (GPa)	Poisson's Ratio	Yield Stress (MPa)	Saturation Stress (MPa)	Saturation Strain
Tension	168.11	0.20	35.00	335.27	0.00703
Compression	168.11	0.20	335.29	959.38	----------
Shear	64.00	------	32.00	182.00	0.00550

TABLE 2.—MATERIAL CONSTANTS FOR CONSTITUTIVE EQUATIONS

D_o	n	Z_1 MPa	Z_o MPa	q	α_1	α_o	β_1	β_o	κ
1×10^6	1.91	1374.96	150.23	1000.50	0.278	0.468	2.484	1.308	3.00

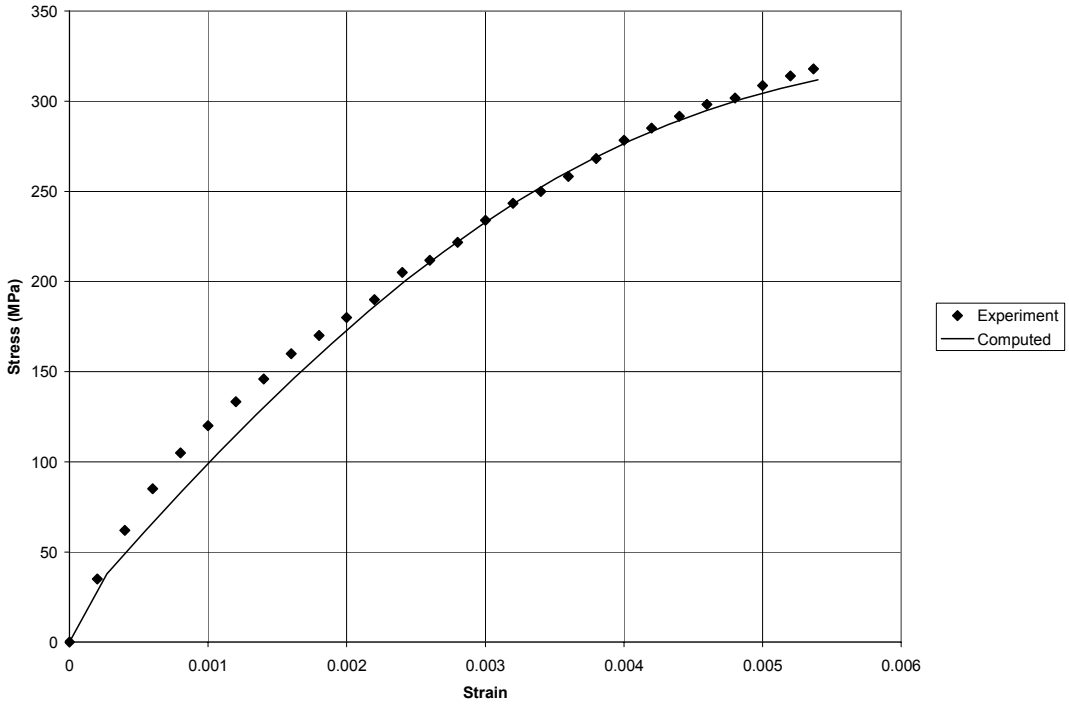

Figure 1.—Experimental and computed tensile stress-strain curves for woven SiC/SiC composite under quasi-static loading conditions.

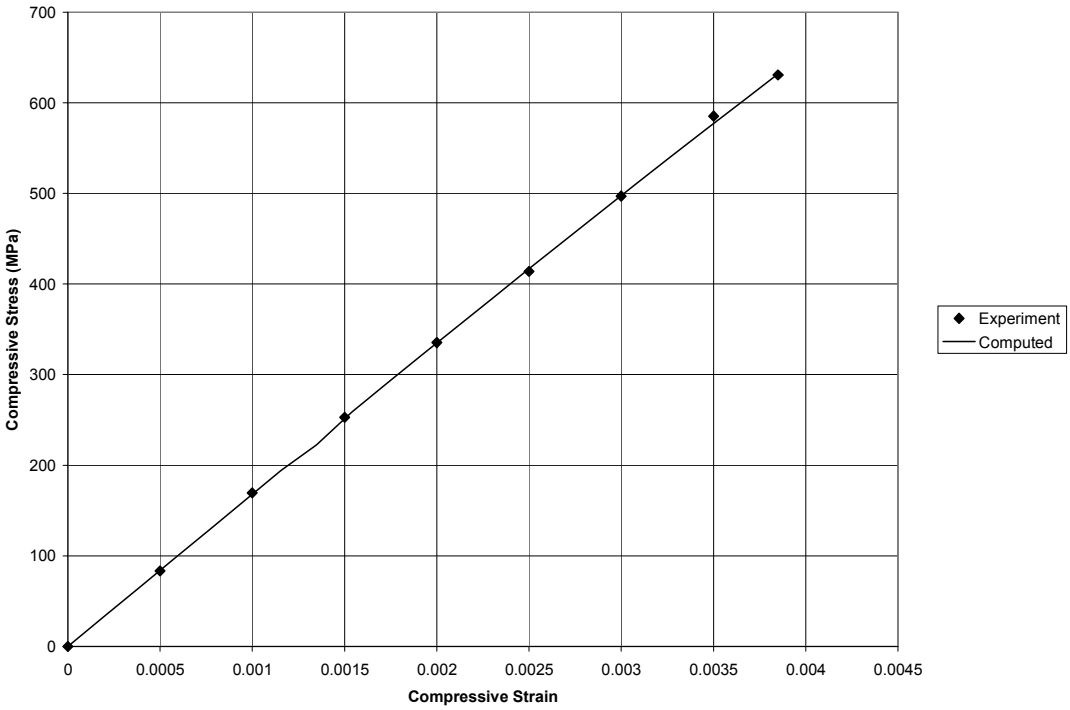

Figure 2.—Experimental and computed compressive stress-strain curves for woven SiC/SiC composite under quasi-static loading conditions.

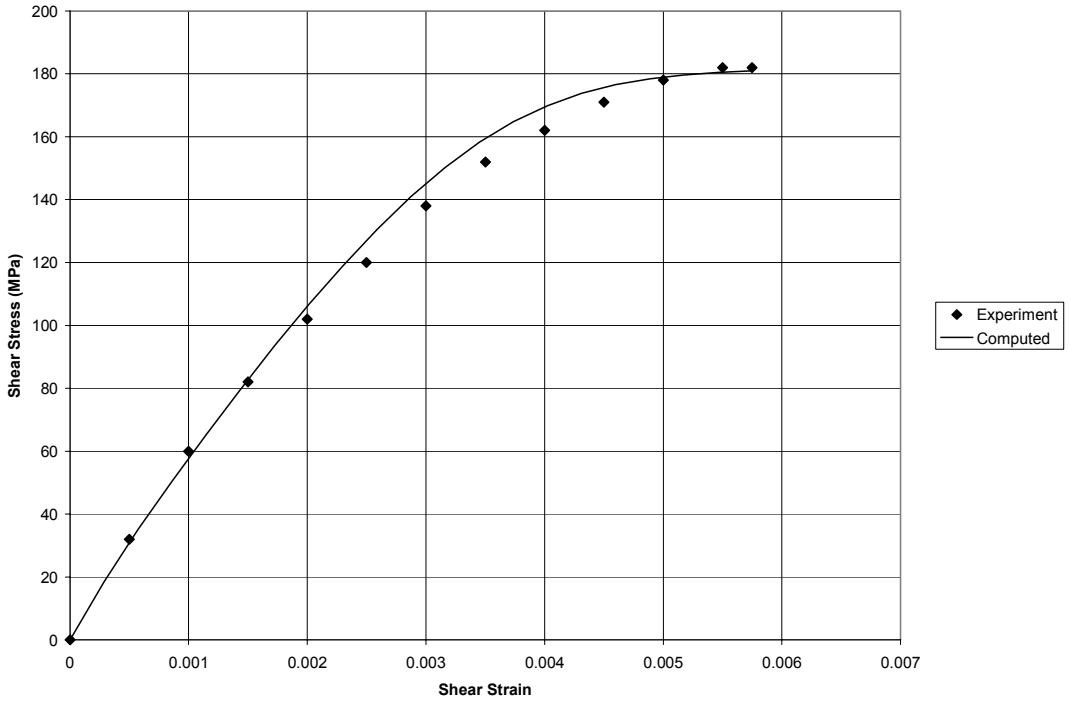

Figure 3.—Experimental and computed shear stress-shear strain curves for woven SiC/SiC composite under quasi-static loading conditions.

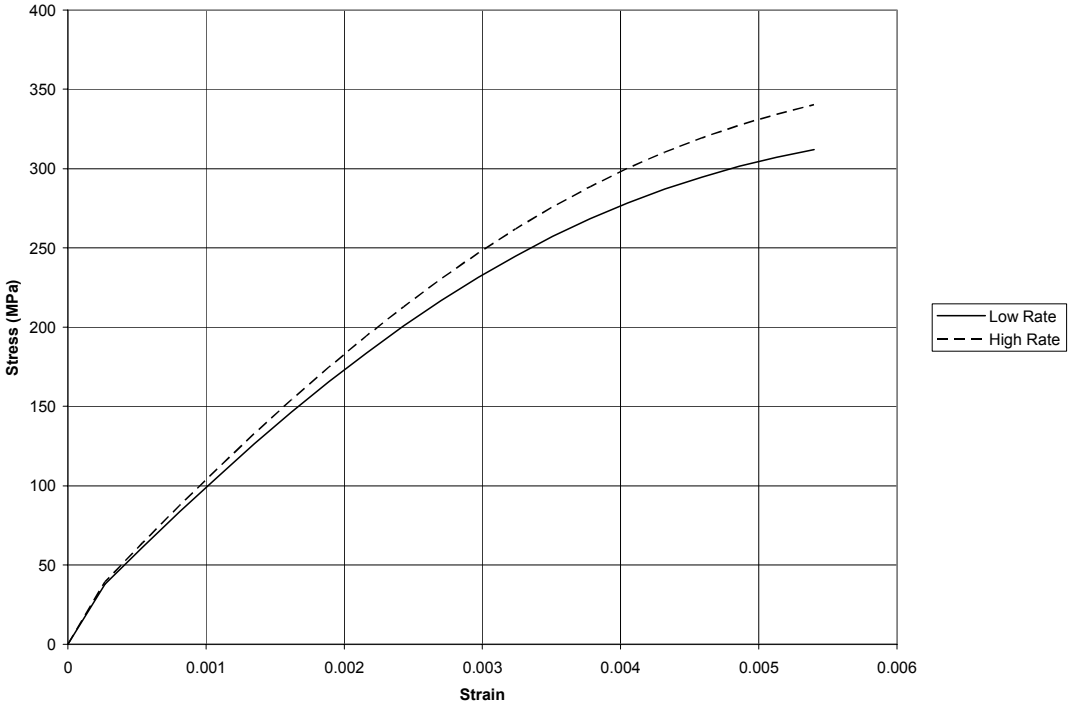

Figure 4.—Computed tensile stress-strain curves of woven SiC/SiC composite at strain rates of 5 x 10^{-5} /sec (Low Rate) and 0.1 /sec (High Rate).

REPORT DOCUMENTATION PAGE

Form Approved
OMB No. 0704-0188

1. AGENCY USE ONLY (*Leave blank*)	2. REPORT DATE	3. REPORT TYPE AND DATES COVERED
	June 2004	Technical Memorandum

4. TITLE AND SUBTITLE

Modeling the Nonlinear, Strain Rate Dependent Deformation of Woven Ceramic Matrix Composites With Hydrostatic Stress Effects Included

5. FUNDING NUMBERS

WBS–22–376–70–30–02

6. AUTHOR(S)

Robert K. Goldberg and Kelly S. Carney

7. PERFORMING ORGANIZATION NAME(S) AND ADDRESS(ES)

National Aeronautics and Space Administration
John H. Glenn Research Center at Lewis Field
Cleveland, Ohio 44135–3191

8. PERFORMING ORGANIZATION REPORT NUMBER

E–14619

9. SPONSORING/MONITORING AGENCY NAME(S) AND ADDRESS(ES)

National Aeronautics and Space Administration
Washington, DC 20546–0001

10. SPONSORING/MONITORING AGENCY REPORT NUMBER

NASA TM—2004-213125

11. SUPPLEMENTARY NOTES

Responsible person, Robert K. Goldberg, organization code 5920, 216–433–3330.

12a. DISTRIBUTION/AVAILABILITY STATEMENT

Unclassified - Unlimited
Subject Category: 24 Distribution: Nonstandard

Available electronically at http://gltrs.grc.nasa.gov

This publication is available from the NASA Center for AeroSpace Information, 301–621–0390.

12b. DISTRIBUTION CODE

13. ABSTRACT ***(Maximum 200 words)***

An analysis method based on a deformation (as opposed to damage) approach has been developed to model the strain rate dependent, nonlinear deformation of woven ceramic matrix composites with a plain weave fiber architecture. In the developed model, the differences in the tension and compression response have also been considered. State variable based viscoplastic equations originally developed for metals have been modified to analyze the ceramic matrix composites. To account for the tension/compression asymmetry in the material, the effective stress and effective inelastic strain definitions have been modified. The equations have also been modified to account for the fact that in an orthotropic composite the in-plane shear stiffness is independent of the stiffness in the normal directions. The developed equations have been implemented into a commercially available transient dynamic finite element code, LS-DYNA, through the use of user defined subroutines (UMATs). The tensile, compressive, and shear deformation of a representative plain weave woven ceramic matrix composite are computed and compared to experimental results. The computed values correlate well to the experimental data, demonstrating the ability of the model to accurately compute the deformation response of woven ceramic matrix composites.

14. SUBJECT TERMS

Composite materials; Ceramic matrix composites; Strain rate; Impact; Constitutive equations

15. NUMBER OF PAGES

19

16. PRICE CODE

17. SECURITY CLASSIFICATION OF REPORT	18. SECURITY CLASSIFICATION OF THIS PAGE	19. SECURITY CLASSIFICATION OF ABSTRACT	20. LIMITATION OF ABSTRACT
Unclassified	Unclassified	Unclassified	